ALN-BASED PIEZOELECTRIC MICROPOWER GENERATOR FOR LOW AMBIENT VIBRATION ENERGY HARVESTING

C. Schröder[*], F. Stoppel, B. Wagner, W. Benecke
Fraunhofer Institute for Silicon Technology ISIT, Itzehoe, Germany
*Presenting Author: Christian.Schroeder@isit.fraunhofer.de

Abstract: In this paper a resonant micropower generator, based on the transverse piezoelectric effect, is presented. The generator consists of a bulk silicon mass, attached to a polysilicon cantilever covered with an AlN thinfilm as piezoelectric material. To maximize the power density of the generator, a parametric study by means of analytical modeling and FEM simulation has been performed. Different optimized generators with resonance frequencies in the range from 100 Hz up to 1 kHz have been designed and fabricated, using dedicated MEMS technology processes. First unpackaged prototypes showed a quality factor of about 500 at atmospheric pressure and were able to generate an electrical output power of up to 1.9 µW at an external acceleration of 1.6 m/s².

Keywords: piezoelectric, micropower, generator, energy, harvesting, AlN, polysilicon

INTRODUCTION

From the beginning of research within the field of micro energy harvesting, a lot of work on piezoelectric generators has been done. Most of this work is focussing on PZT as piezoelectric material, due to its high piezoelectric coefficients [1,2]. Since the generator performance also strongly depends on the permittivity and the Young's modulus of the piezoelectric material, AlN is a suitable alternative to PZT, offering a good compatibility to MEMS processes and overcoming the need for special polarization treatments [3,4]. To examine maximum power densities of AlN-based and PZT-based generators, a simple generator configuration consisting of a bulk silicon mass, attached to a polysilicon cantilever covered with metal electrodes and a piezoelectric thinfilm has been investigated.

THEORY
Analytical Modeling

The dynamic behavior of the generator is described by a novel bidirectional coupled segmented analytical model, assuming a damped harmonic oscillator with an effective mass of m_{eff}, being excited by an external acceleration a. Since the piezoelectric material generates an additional restoring force due to the inverse piezoelectric effect, the well known equation of motion for those oscillators has to be extended by an additional coupling term, resulting in Eq. 1. Therein z_M denotes the deflection of the mass, c the viscous damping constant, K the effective stiffness of the cantilever and the mass, d_{31} the transverse piezoelectric coefficient and U the generated voltage. The factors β and ξ are depending on the geometry of the mass, the electrodes and the cantilever as well as the Young's modulus Y and the position of the neutral axis z_n within the cantilever, see Eq. 2, Eq. 3 and Eq. 4. For simplicity thin layers like the electrodes and the insulators are neglected. Furthermore the mass is assumed to be a single silicon layer with the height h_M, see Fig. 1.
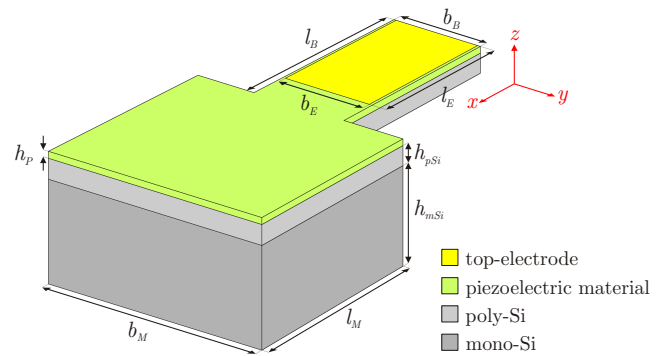

Fig. 1: Dimensions used for analytical modeling and FEM simulation with different lengths l, widths b and heights h.

To determine the deflection z_M and the effective stiffness K, the curvature of the cantilever and the mass as a function of the acting force is calculated from the appearing moments and the position of each neutral axis. Double integration and combination of these terms using adequate boundary conditions leads to the deflection z_M of the mass in its centre point, which related to the acting force yields in Eq. 5.

By applying the fundamental equation for the direct piezoelectric effect and Kirchhoff's laws with respect to the geometry of the cantilever the generated current i_P can be derived. Transformation into the frequency domain, taking into account Eq. 1 and Eq. 5, gives an expression for the generated power P on a load resistance R, see Fig. 2, with ω and j denoting the angular frequency and the imaginary unit, see Eq. 6.

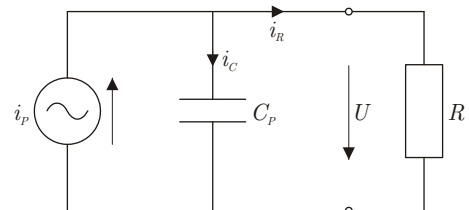*Fig. 2: Equivalent circuit model with piezoelectric current source i_P, piezoelectric capacitance C_P, load resistance R and voltage U.*

$$m_{eff}\, a = -m_{eff}\, \frac{\mathrm{d}^2}{\mathrm{d}t^2}z_M - c\,\frac{\mathrm{d}}{\mathrm{d}t}z_M - z_M\, K + \frac{d_{31}\, Y_P\, U}{\beta\, h_P} \quad \text{with} \quad m_{eff} \approx m_M + \tfrac{33}{140}m_B \tag{1}$$

$$\beta = 2\,\xi_B\left(\frac{l_M}{2} - \frac{l_E}{2} + l_B\right)\left(\frac{h_P}{2} + z_n\right)Y_P \tag{2}$$

$$\xi_B = \frac{6h_{pSi}Y_{pSi} + 6h_P Y_P}{b_B\left(h_{pSi}^4 Y_{pSi}^2 + 4h_P h_{pSi}\left(h_{pSi}^2 + \frac{3h_P h_{pSi}}{2} + h_P^2\right)Y_P Y_{pSi} + h_P^4 Y_P^2\right)} \tag{3}$$

$$\xi_M = \frac{6}{b_M\, h_M^3\, Y_{mSi}} \quad \text{with} \quad h_M = h_{mSi} + h_{pSi} + h_p \tag{4}$$

$$K = \frac{12}{\xi_M\, l_M^3 + 6\,\xi_B\, l_B\, l_M^2 + 12\,\xi_B\, l_B^2\, l_M + 8\,\xi_B\, l_B^3} \tag{5}$$

$$P = \left|\frac{j\,\omega\, d_{31}\,\beta\, m_{eff}\, a\, b_E\, l_E\, K\, h_P}{\left(j\,\omega\, d_{31}^2\, b_E\, l_E\, K\, Y_P + \left(j\,\omega\, K - j\,\omega^3\, m_{eff} - \omega^2 c\right)h_P\, C_P\right)R + \left(K - \omega^2\, m_{eff} + j\,\omega c\right)h_P}\right|^2 R \tag{6}$$

Parametric study

Using the described analytical model, a detailed parametric study has been performed, showing that AlN-based generators are able to generate a comparable output power as PZT-based generators, although the transverse piezoelectric coefficient of AlN $d_{31} \approx$ -2.9 pC/N is very low compared to the piezoelectric coefficient of PZT $d_{31} \approx$ -100 pC/N. This is mainly due to the low dielectric constant of AlN, which is in the range of 10 to 11 and more than 100 times smaller than the dielectric constant of PZT. Additionally, AlN has a four times higher Young's modulus of about 345 GPa, leading to higher mechanical stress under deflection. Since the Young's modulus of the piezoelectric material also strongly influences the position of the neutral axis, the optimum AlN thickness for maximum output power is about a factor of three smaller than the corresponding PZT thickness, see Fig. 3.
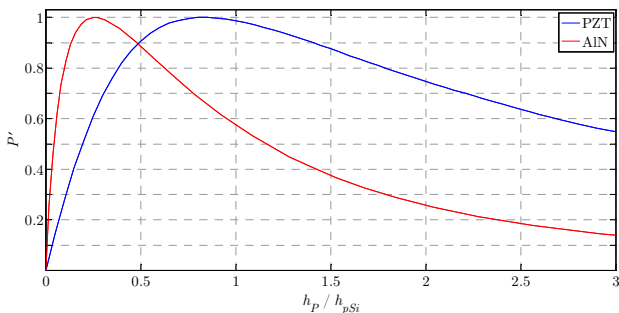

Fig. 3: Normalized power density P' as a function of the layer thickness ratio h_p / h_{pSi} at constant resonance frequency.

As an effect of the bidirectional coupling the parametric study reveals that the maximum deflection decreases and the resonance frequency increases with increasing piezoelectric coefficients $|d_{31}|$, enabling the generator to convert more kinetic energy into electrical energy, see Fig. 4.
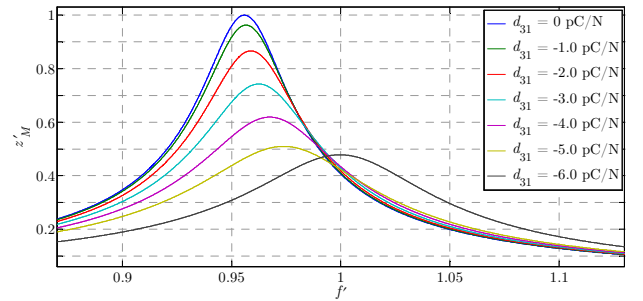

Fig. 4: Normalized deflection z'_M as a function of the normalized frequency f' and the piezoelectric coefficient d_{31} at optimal load resistance.

A further improvement can be achieved by using short cantilevers and larger masses, optimizing the mass per volume.

FEM simulation

For the investigation of more complex cantilever and electrode geometries, additional FEM simulations have been done. They indicate that the output power increases and the voltage decreases as the electrode coverage of the cantilever is increased, see Fig. 5. This is caused by nonuniform mechanical stress profiles and electromechanical back coupling, getting worse for larger electrodes.
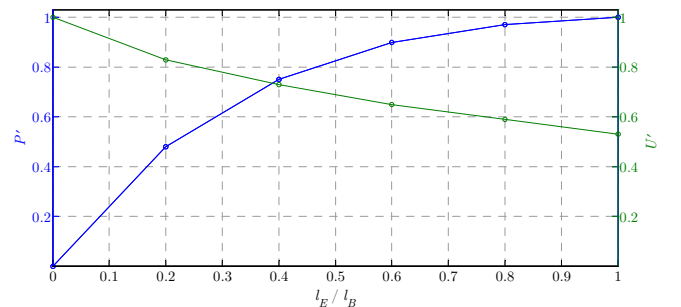

Fig. 5: Normalized power density P' and voltage U' as a function of the electrode coverage l_E / l_B.

A reduction of the back coupling can be achieved by optimizing the cantilever shape with respect to a more uniform mechanical stress profile. Due to that trapezoidal shaped cantilevers are able to generate up to 20 % higher output powers as rectangular shaped cantilevers, see Fig. 6.
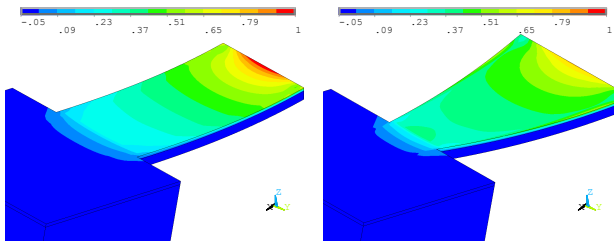

Fig. 6: Normalized electrical potential for rectangular shaped cantilevers (left) and trapezoidal shaped cantilevers (right).

EXPERIMENTAL
Design and fabrication

Based on the results of the parametric study and the FEM simulations, 16 optimized generator designs including rectangular and trapezoidal shaped cantilevers, different electrode coverage and resonance frequencies of 100 Hz, 250 Hz, 500 Hz and 1 kHz have been created, see Fig 7.
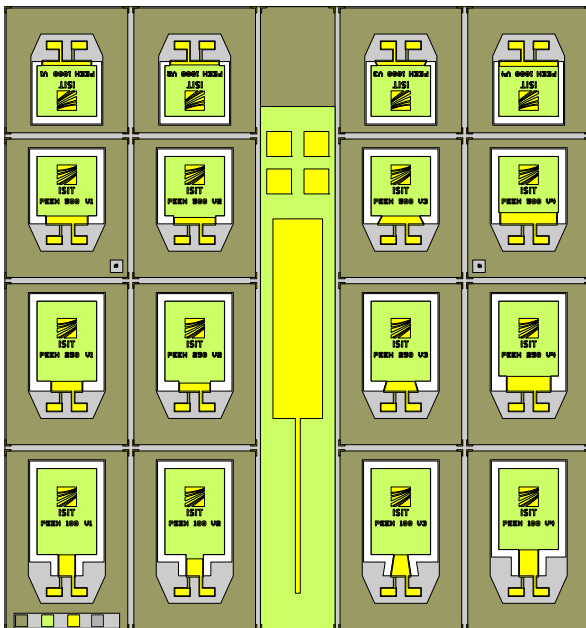

Fig. 7: Reticle with piezoelectric teststructures and different generator designs varying in resonance frequency, cantilever geometry and electrode coverage.

The corresponding mask set leads to a process flow comprising five lithographic layers, see Fig. 8. For the fabrication of first AlN-based prototypes a 200 mm SOI wafer with an 11.5 µm thick polysilicon devicelayer was used. After depositing a 1 µm thick LPCVD SiO2 isolation layer, a Ti/Pt bottom-electrode is evaporated and lift-off patterned. This is followed by magnetron sputtering of a 2 µm thick AlN piezo-electric thinfilm, being structured by TMAH wet etching using a molybdenum hardmask. After realizing a sputtered Cr/Au top-electrode the cantilever and the mass are defined by double-sided DRIE and released by HF gas-phase etching.
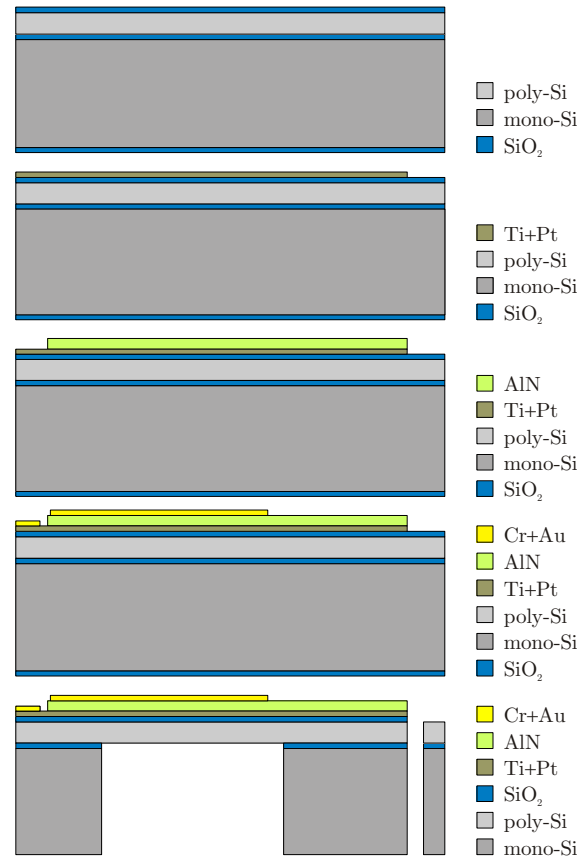

Fig. 8: Process flow (from top to bottom): LPCVD of SiO_2 isolation; evaporation and lift-off of Ti/Pt bottom-electrode; sputtering and etching of AlN piezoelectric thinfilm; sputtering and etching of Cr/Au top-electrode; DRIE and gas phase release of polysilicon cantilever and bulk silicon mass.

Characterization

First unpackaged generator prototypes with 2 µm thick AlN and resonance frequencies of 100 Hz and 250 Hz have been characterized under ambient atmosphere. Therefore they were assembled on PCB, mounted on an electromagnetic shaker and connected to their optimal load resistance, see Fig. 9.
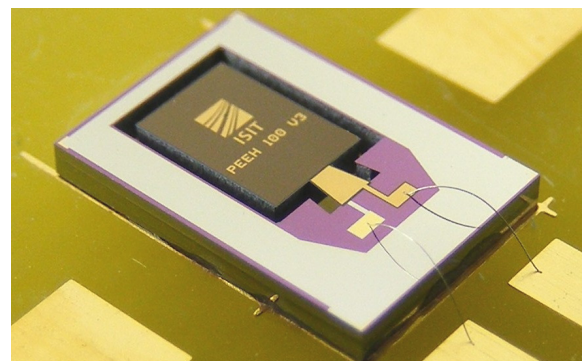

Fig. 9: Assembled generator prototype with a trapez-oidal shaped cantilever and a chipsize of 5×7.2 mm².

By applying a sinusoidal oscillation at varying frequency and different accelerations, the voltage generated on the load resistance has been measured. Prototypes designed for 100 Hz resonance frequency were able to generate an output power of about 0.8 μW at 105.6 Hz, 1 m/s² and 21 MΩ, showing a slightly nonlinear frequency response at larger deflections, see Fig. 9.
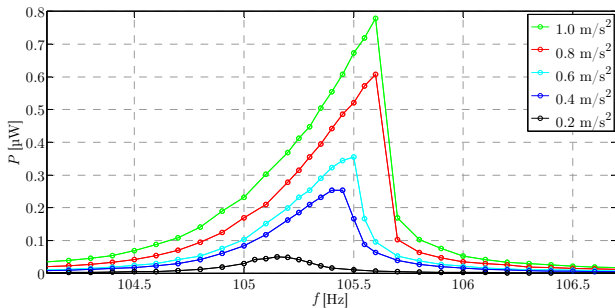

Fig. 9: Measured output power P of a 100 Hz prototype as a function of the frequency f and different accelerations at constant load resistance of 21 MΩ.

Prototypes designed for 250 Hz resonance frequency were able to generate an output power of about 1.9 μW at 259.8 Hz, 1.6 m/s² and 5 MΩ, achieving a quality factor of about 500, see Fig. 10.
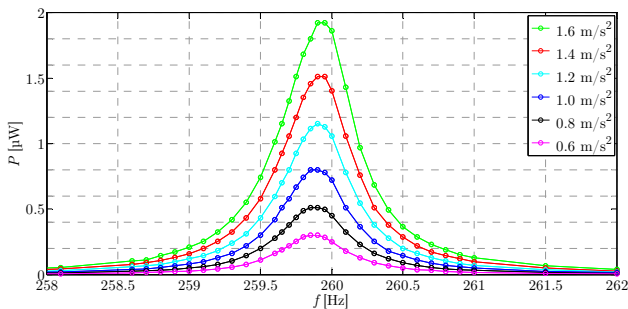

Fig. 10: Measured output power P of a 250 Hz prototype as a function of frequency f and different accelerations at constant load resistance of 5 MΩ.

CONCLUSION

Resonant micropower generators, based on the transverse piezoelectric effect, have been investigated by means of analytical modeling and FEM simulation. As the result of a detailed parametric study it could be shown, that AlN is a suitable alternative to PZT as piezoelectric material, being able to generate a comparable output power, offering a good compatibility to MEMS processes and overcoming the need for special polarization treatments. Different optimized generator designs with resonance frequencies in the range from 100 Hz up to 1 kHz have been fabricated, using a five lithographic layer comprising MEMS process flow. First unpackaged prototypes showed a quality factor of about 500 under atmospheric pressure and were able to generate an electrical output power of up to 1.9 μW at an external acceleration of 1.6 m/s².

REFERENCES

[1] Beeby SP, Tudor MJ, White NM 2006 Energy harvesting vibration sources for microsystems applications *Measurement Science and Technology* **17** R175–195

[2] Anton SR, Sodano HA 2007 A review of power harvesting using piezoelectric materials (2003–2006). *Smart Materials and Structures* **16** R1–21

[3] Elfrink R, Kamel TM, Goedbloed M, Matova S, Hohlfeld D, van Schaijk R et al. 2008 Vibration energy harvesting with aluminum nitride based piezoelectric devices *Technical Digest Power MEMS (Sendai, Japan, 9-12 November 2008)* 249–52

[4] Marzencki M, Ammar Y, Basrour S 2008 Integrated power harvesting system including a MEMS generator and a power management circuit *Sensors & Actuators A: Physical* **145** 363–370